[CANCER RESEARCH 64, 7486–7490, October 15, 2004]

Adeno-Associated Viral Vector-Mediated Expression of Endostatin Inhibits Tumor Growth and Metastasis in an Orthotropic Pancreatic Cancer Model in Hamsters

Takuji Noro,[1,3] Koichi Miyake,[1] Noriko Suzuki-Miyake,[1] Tsutomu Igarashi,[1] Eiji Uchida,[2] Takeyuki Misawa,[3] Yoji Yamazaki,[3] and Takashi Shimada[1]

Departments of [1]Biochemistry and Molecular Biology and [2]Surgery for Organ Function and Biological Regulation, Nippon Medical School, Tokyo, Japan; and [3]Department of Surgery, Jikei University School of Medicine, Tokyo, Japan

ABSTRACT

We examined the feasibility of using adeno-associated virus (AAV)-mediated systemic delivery of endostatin in gene therapy to treat metastasis of pancreatic cancer. We established an animal model of orthotopic metastatic pancreatic cancer in which the pancreatic cancer cell line PGHAM-1 was inoculated into the pancreas of Syrian golden hamsters. Transplanted cells proliferated rapidly and metastasized to the liver. An AAV vector expressing endostatin (5×10^{10} particles) was injected intramuscularly into the left quadriceps or intravenously into the portal vein. These routes of vector administration were evaluated by comparing various parameters of tumor development. Intramuscular injection of the vector modestly increased the serum endostatin level. The numbers of metastases and the incidence of hemorrhagic ascites were decreased in the treated animals. In contrast, the serum concentration of endostatin was significantly increased after intraportal injection of the vector. The antitumor effects on all parameters (including the size and microvessel density of primary pancreatic tumors, the sizes and number of liver metastases, and the incidence of hemorrhagic ascites) were significant. These results suggest that systemic delivery of endostatin represents a potentially effective treatment for pancreatic cancer and liver metastases. The route of vector administration influences the efficacy of AAV-mediated endostatin expression. Intraportal injection of the AAV vector appears to be more effective as an antiangiogenic gene therapy for pancreatic cancer.

INTRODUCTION

Pancreatic cancer is characterized by local invasion of adjacent structures and early metastasis to the liver and lymph nodes. Because of difficulties in early diagnosis and effective treatment, pancreatic cancer is often lethal (1). Local recurrence occurs in up to 85% of patients who undergo the currently available modality of surgical treatment (2). Despite extensive surgery, chemotherapy, and radiotherapy, the 5-year survival rate for patients with pancreatic cancer remains very low (3). Furthermore, the incidence of pancreatic cancer in the West has increased over the last four decades (4), indicating a pressing need for novel strategies that are effective against primary pancreatic cancer and the resultant liver metastases.

Gene therapy is an important option under active investigation for cancer therapy, although no definitive clinical efficacy has yet been demonstrated (5). Among a number of possible approaches, systemic gene therapy appears to be preferable for both inhibiting tumor growth and preventing metastases. The efficacy of systemic immunogene therapy using various cytokine genes has been demonstrated in various animal models (6–8). An alternative approach is the use of antiangiogenic genes. Because the neovasculature is essential for tumor growth and metastasis, the inhibition of angiogenesis is a promising anticancer strategy (9, 10).

Received 4/29/03; revised 7/6/04; accepted 8/20/04.

Grant support: A grant from the Ministry of Health and Welfare of Japan and the Ministry of Education, Science and Culture of Japan.

The costs of publication of this article were defrayed in part by the payment of page charges. This article must therefore be hereby marked *advertisement* in accordance with 18 U.S.C. Section 1734 solely to indicate this fact.

Requests for reprints: Takashi Shimada, Department of Biochemistry and Molecular Biology, Nippon Medical School, 1-1-5 Sendagi Bunkyo-ku, Tokyo 113-8602, Japan. E-mail: tshimada@nms.ac.jp.

The present study examines the feasibility of antiangiogenic gene therapy for treatment of pancreatic cancer using an orthotopic model. When PGHAM-1 derived from chemically induced hamster pancreatic cancer cells (11) is injected into the pancreas of hamsters, the cells develop ductal adenocarcinoma that closely resembles human pancreatic carcinoma and, like its human counterpart, frequently metastasizes to the liver. Thus, hamsters inoculated with PGHAM-1 cells represent an orthotopic pancreatic cancer model (12).

We used a classical adeno-associated virus (AAV) serotype 2 vector expressing endostatin to achieve a systemic state of antiangiogenesis in model animals. Endostatin is a 20-kDa COOH-terminal fragment of collagen and exerts powerful antiangiogenic activity through inhibition of endothelial cell proliferation and migration (13–15). The AAV vector is known to be particularly useful for long-term expression of transgenes in muscle, liver, and brain cells (16–19). Therefore, we compared the intramuscular and intraportal routes of AAV vector administration in terms of systemic endostatin expression.

MATERIALS AND METHODS

Plasmid Construction and Vector Production. The helper plasmid containing the complete AAV genome (psub201) and the AAV serotype 2 packaging plasmid (pAAV/Ad) have been described previously (20). The soluble mouse endostatin expression unit was constructed essentially as described previously (21). Briefly, mouse endostatin cDNA was amplified by reverse transcription-polymerase chain reaction from total liver RNA using the oligonucleotide primers 5′-GCGGATCCCATACTCATCAGGACTTTCAGCCA-3′ and 5′-GCCTCGAGCTATTTGGAGAAAGAGGTCATGAA-3′ and inserted into pHook1 (Invitrogen, Carlsbad, CA) to generate pHK-ES, in which the coding sequences for a murine immunoglobulin κ signal peptide and influenza virus hemagglutinin A epitope located upstream of the endostatin gene. The coding sequence for immunoglobulin κ-hemagglutinin A-endostatin was then cloned as an *Eco*RI-*Eco*RI fragment into the AAV plasmid containing the CAG promoter and the enhanced green fluorescence protein (*EGFP*) gene driven by the B19 promoter (22). We generated pAAV-EGFP containing the EGFP gene driven by the CAG promoter as a control.

AAV vectors (AAV-End and AAV-EGFP) were generated by adenovirus-dependent transfection and concentrated by sulfonated cellulose column chromatography (Seikagaku Kougyou, Tokyo, Japan) and filtration with Centriprep YM 10 (Millipore, Bedford, MA) as described previously (23). The genome titer of the AAV vector was determined by slot blot hybridization with the endostatin probe.

***In vitro* Tube Formation Assay.** To evaluate the antiangiogenic activity of AAV-End, *in vitro* tube formation assay was performed using an angiogenesis kit (Krabo, Okayama, Japan) as described previously (24). Briefly, human umbilical vein endothelial cells (HUVECs) cocultured with human fibroblasts were transduced with AAV-End or AAV-EGFP (1×10^{10} particles per mL) and cultured in medium containing vascular endothelial growth factor (VEGF). After 10 days, fixed cells were incubated with mouse antihuman CD31 (Kurabo, Okayama, Japan) and stained with metal-enhanced 3,3′-diaminobenzidine tetrahydrochloride. The total area and tube length were quantified using an angiogenesis image analyzer (Kurabo) and then statistically analyzed with Student's *t* test.

Animal Experiments. Syrian golden hamsters were obtained from the Shizuoka Laboratory Animal Center (Shizuoka, Japan). All animal experiments proceeded according to the regulations established by the Ethical Committee of Nippon Medical School.

An orthotopic pancreatic cancer model was established according to the

methods described by Matsushita *et al.* (12). The PGHAM-1 cell line (the hamster pancreatic cancer cell line) was derived from hamster pancreatic cancer cells induced with *N*-nitrosobis(2-oxopropyl)amine (12). Hamsters were anesthetized with Nembutal and then underwent laparotomy. Suspensions of 5×10^6 PGHAM-1 cells were injected into the splenic lobe of the pancreas using a 29-gauge needle, and then the abdominal wall was closed (12).

AAV vectors were injected into 4-week-old female Syrian golden hamsters 21 days before implantation of PGHAM-1 cells. In one group, AAV-End vector genomes (0.5 or 1.5×10^{11} particles) in a total volume of 100 μL suspended in PBS were injected into the left quadriceps muscle after anesthetization with diethyl ether. In another group, the same dose of AAV-End was injected into the portal veins of 4-week-old anesthetized hamsters as follows. The intestine was displaced through an upper middle incision, and then the portal vein was exposed. The hamsters were treated with a single bolus injection of AAV-End vector genomes in a total volume of 100 μL via a 30-guage needle. The abdomen was then sutured layer to layer using 4-0 silk. Control hamsters received intramuscular or intraportal injection with PBS or AAV-EGFP. On day 0, 5×10^6 PGHAM-1 cells were implanted in the hamster pancreas. Twenty-one days after the surgical implantation of PGHAM-1 cells, hamsters were anesthetized and humanely killed. The liver and pancreas were removed from each hamster, and the volume of the primary pancreatic tumor, the number of liver metastases, and the diameter of the largest liver metastasis were assessed. The volume (V) of the primary tumor was calculated from the following formula: $V = a^2 \times b \times 0.52$ (where a is the shortest diameter and b is the longest diameter). At the end of each experiment, the organs of these hamsters were fixed in 4% paraformaldehyde and embedded. Portions of these organs were preserved at −80°C. In addition, the heart, lungs, pancreas, and kidneys of tumor-bearing hamsters were histologically examined.

Enzyme-Linked Immunosorbent Assay. Blood samples were collected by cardiocentesis of ether-anesthetized hamsters. Serum endostatin concentrations were determined using a murine endostatin enzyme-linked immunosorbent assay (ELISA) kit (ACCUCYTE murine endostatin; CytImmune Sciences, College Park, MD) according to the manufacturer's instructions.

Polymerase Chain Reaction Analysis. To evaluate the distribution of AAV-End after intramuscular and intraportal injection, 800 μg of genomic DNA were extracted from each organ of the hamsters and analyzed by polymerase chain reaction (PCR) using primers that amplified a 277-bp region derived from the *EGFP* gene. The primers were 5′-CAGCCGCTACCCCGACCACA-3′ (sense) and 5′-CACCTTGATGCCGTTCTTCT-3′ (antisense). PCR conditions were as follows: 94°C for 5 minutes; 30 cycles of 94°C for 30 seconds, 58°C for 30 seconds, and 72°C for 1 minute; and 72°C for 5 minutes. Integrity of DNA was determined by amplifying a 661-bp region of the β-actin gene using the appropriate primers (5′-GACGGGGTCACCCACACTGTGCCCATCTA-3′ and 5′-CTAGAAGCATTTGCGGTGGACGATGG-3′).

Histologic and Immunohistochemical Examination. Sections were immunohistochemically stained using streptavidin biotin as described previously (11, 12). Paraffin sections (3 μm) were cut for immunostaining with von Willebrand factor as follows. Deparaffinized tissue sections were digested with Pronase (DAKO Japan Co., Kyoto, Japan) for 10 minutes before exposure to rabbit polyclonal antibody against von Willebrand factor (DAKO Japan Co.), and subsequent steps were carried out with a MAX-PO(R) kit (Nichirei Co., Tokyo, Japan) according to the manufacturer's instructions. Sections were counterstained with hematoxylin. Microvessels were detected by substrate reaction with diaminobenzidine. The areas of the tumor with the highest microvessel density were identified, and microvessels were counted under ×200 magnification. At least three fields were counted per animal, and the average was taken as the microvessel density of each pancreatic tumor.

Statistical Analysis. Student's t test was used to analyze statistical differences between each group in terms of volume of primary tumor, number of liver metastases, diameter of the largest liver metastatic tumor, and microvessel density. Incidence rate of hemorrhagic ascites was analyzed by χ^2 test and the correction formula of Yates.

RESULTS

AAV Vector-Mediated Expression of Endostatin *In vitro*. We generated an AAV vector containing the secretable form of the murine endostatin gene driven by the CAG promoter (AAV-End). Assays of *in vitro* tube formation using HUVECs cocultured with fibroblasts confirmed the AAV-mediated expression of biologically active endostatin. In the presence of VEGF, HUVECs generated tube-like structures (Fig. 1*A*). Transduction with a control AAV-EGFP vector did not affect tube formation (Fig. 1*B*). However, the number of tubes in cells transduced with AAV-End was significantly reduced (Fig. 1*C*). Measurements of tube area (Fig. 1*D*) and length (Fig. 1*E*) confirmed that AAV-End was able to inhibit *in vitro* angiogenesis.

Generation of a Hamster Pancreatic Cancer Model. We generated an orthotopic model of pancreatic cancer by direct inoculation of PGHAM-1 cells into the splenic lobe of the pancreas. The inoculated cells proliferated rapidly and formed a mass in all animals approximately 7 days after transplantation. Metastases to the liver were observed in all animals after 3 weeks. Most of the hamsters bearing transplanted tumors developed massive hemorrhagic ascites. All of the transplant-treated animals died around 4 weeks after transplantation due to advanced tumor growth and metastases.

AAV Vector-Mediated Expression of Endostatin in Syrian Golden Hamsters with Pancreatic Tumors. In the first experiment, we measured the concentrations of serum endostatin after intramuscular or intraportal injection of AAV-End (0.5 or 1.5×10^{11} particles; Fig. 2*A*). The background level of serum endostatin in control hamsters that received intramuscular injection of PBS was 18.3 to 33.3 ng/mL. In accordance with previous reports (25, 26), AAV vector-

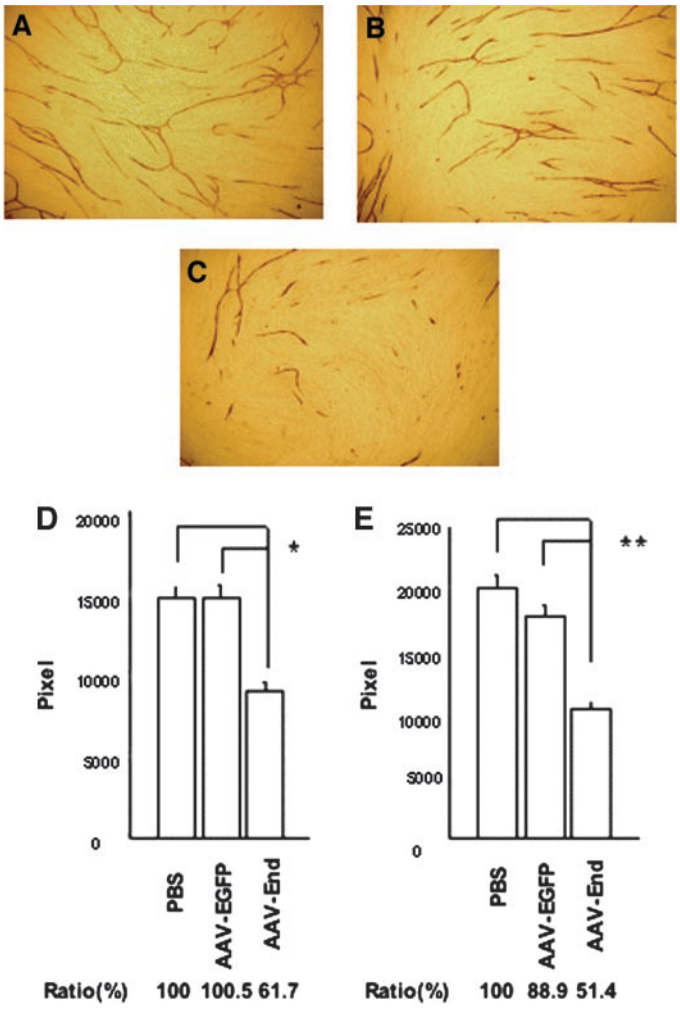

Fig. 1. Antiangiogenic activity of AAV-End in tube formation assay. HUVECs cocultured with human fibroblasts in the presence of VEGF were incubated with PBS (*A*), AAV-EGFP (*B*), or AAV-End (*C*). The area (*D*) and length (*E*) of tube-like structures were measured quantitatively using an image analyzer. *, $P < 0.05$; **, $P < 0.01$.

mediated gene expression increased gradually, with a peak at 4 to 6 weeks after either intramuscular or intraportal injection. Intramuscular injection moderately increased the serum endostatin level, whereas significantly higher levels of serum endostatin were observed after intraportal injection. A 3-fold increase of the vector dose only slightly raised the serum endostatin level (Fig. 2*A*).

The growth rate of PGHAM-1 cells is very rapid (11, 27). Therefore, to study the antitumor activity of the AAV vector, we injected the AAV vector (0.5×10^{11} particles) 21 days before inoculation with tumor cells. All animals were sacrificed 21 days after transplantation with tumor cells (42 days after vector injection) to allow biochemical and histologic analyses. The concentrations of serum endostatin at autopsy are shown Fig. 2*B*. The background level of serum endostatin (50.8–51.9 ng/mL) was not changed by either laparotomy or intraportal injection of PBS or AAV-EGFP. Intramuscular injection of AAV-End moderately increased the serum endostatin level (124.5 ± 27.0 ng/mL), whereas the level of endostatin expression became significantly higher after intraportal injection (225.5 ± 31.0 ng/mL; Fig. 2*B*).

Distribution of AAV-End was determined by PCR analysis of the *EGFP* sequence, which was derived from the second gene in the AAV-End vector. When AAV-End was injected into the left quadriceps muscle, the EGFP-specific 277-bp fragment was detected only at the injected site. On the other hand, the *EGFP* sequence was detected not only in the liver but also in the kidneys, heart, and pancreas after intraportal injection (Fig. 3*A* and *B*).

Effects on the Growth of the Primary Pancreatic Tumor. We evaluated the growth rate of the primary tumor in the pancreas (Fig. 4*A* and *B*). The average size of the tumor was 395.0 ± 38.8 mm^3. The growth rate was not significantly restricted by intramuscular injection of AAV-End (311.9 ± 66.5 mm^3). In contrast, intraportal administration of AAV-End significantly decreased tumor volume to 174.0 ± 28.0 mm^3.

Tumor sections were stained with an antibody against von Willebrand factor, and the vasculature was subsequently evaluated (Fig. 4*C* and *D*). Microvessel density in the tumor was significantly decreased by AAV-End, irrespective of the injection route. The average vascular density in hamsters that received intramuscular injection with AAV-End was 15.6 ± 2.3 compared with 39.0 ± 6.0 in the control hamsters that received intramuscular injection with AAV-EGFP. The average vascular density in hamsters that received intraportal injection with AAV-End was 6.7 ± 0.9 compared with 36.5 ± 3.5 in the controls that received intraportal injection with AAV-EGFP.

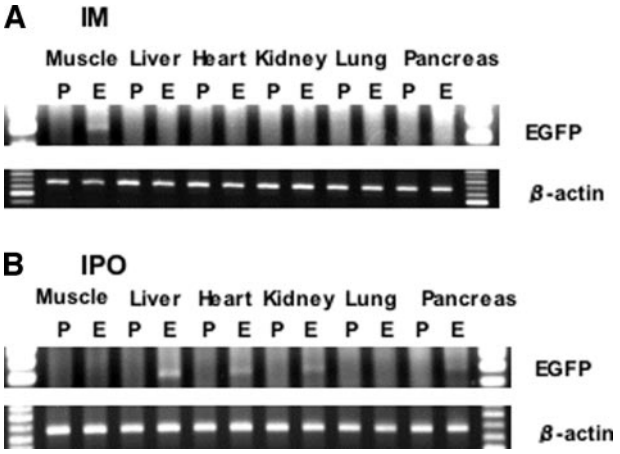

Fig. 3. Vector distribution after *in vivo* administration. PBS (*Lanes P*) or AAV-End (*Lanes E*) was administered through intramuscular (*A*) or intraportal injection (*B*). Genomic DNA was extracted from organs and analyzed by PCR using primers specific for the EGFP gene or β-actin as controls. *IM*, intramuscular injection; *IPO*, intraportal injection.

Effects on Liver Metastasis and Massive Hemorrhagic Ascites. We examined the number and size of the liver metastases (Fig. 5*A*−*C*). Compared with AAV-EGFP, intramuscular injection of AAV-End decreased the number (3.5 *versus* 1.7; $P < 0.05$) but not the size of metastases in the liver, based on maximal diameter (2.2 *versus* 2.8 mm). In contrast, intraportal injection of AAV-End significantly reduced both the number (4.7 *versus* 1.0; $P < 0.01$) and size (3.7 *versus* 0.8 mm; $P < 0.05$) of the metastases.

Massive hemorrhagic ascites are thought to be a parameter of tumor invasion and peritoneal dissemination. Bloody ascites developed in 75.0% (six of eight) of hamsters that received intramuscular injection with AAV-EGFP. Laparotomy followed by intraportal injection with AAV-EGFP slightly increased the incidence rate to 87.5% (seven of eight). The formation of ascites was significantly inhibited after AAV-End injection by either route. The incidence of ascite formation in hamsters that received AAV via intramuscular injection and via intraportal injection was 15.4% (2 of 13) and 18.2% (2 of 11), respectively.

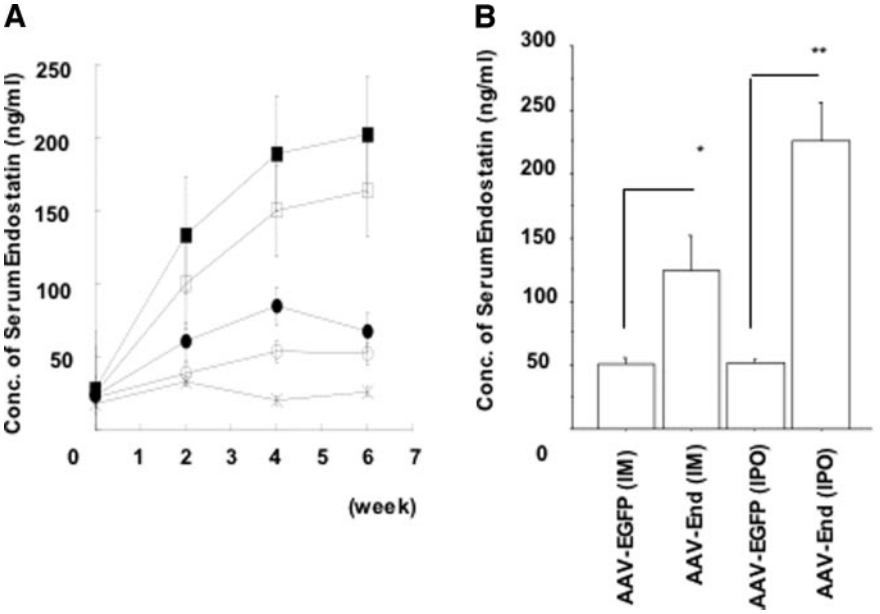

Fig. 2. Serum levels of endostatin after intramuscular or intraportal injection of AAV-End. *A*. AAV-End (0.5 or 1.5×10^{11} particles) was injected intramuscularly or intraportally, and serum concentrations of endostatin were measured every 2 weeks by ELISA. ■, 1.5×10^{11} particles, intraportal injection ($n = 2$); □, 0.5×10^{11} particles, intraportal injection ($n = 2$); ●, 1.5×10^{11} particles, intramuscular injection ($n = 4$); ○, 0.5×10^{11} particles, intramuscular injection ($n = 4$); x, PBS, intramuscular injection ($n = 4$). *B*. Serum endostatin levels were determined by ELISA at autopsy, 42 days after vector administration ($n = 4$). *, $P < 0.05$; **, $P < 0.01$. *IM*, intramuscular injection; *IPO*, intraportal injection.

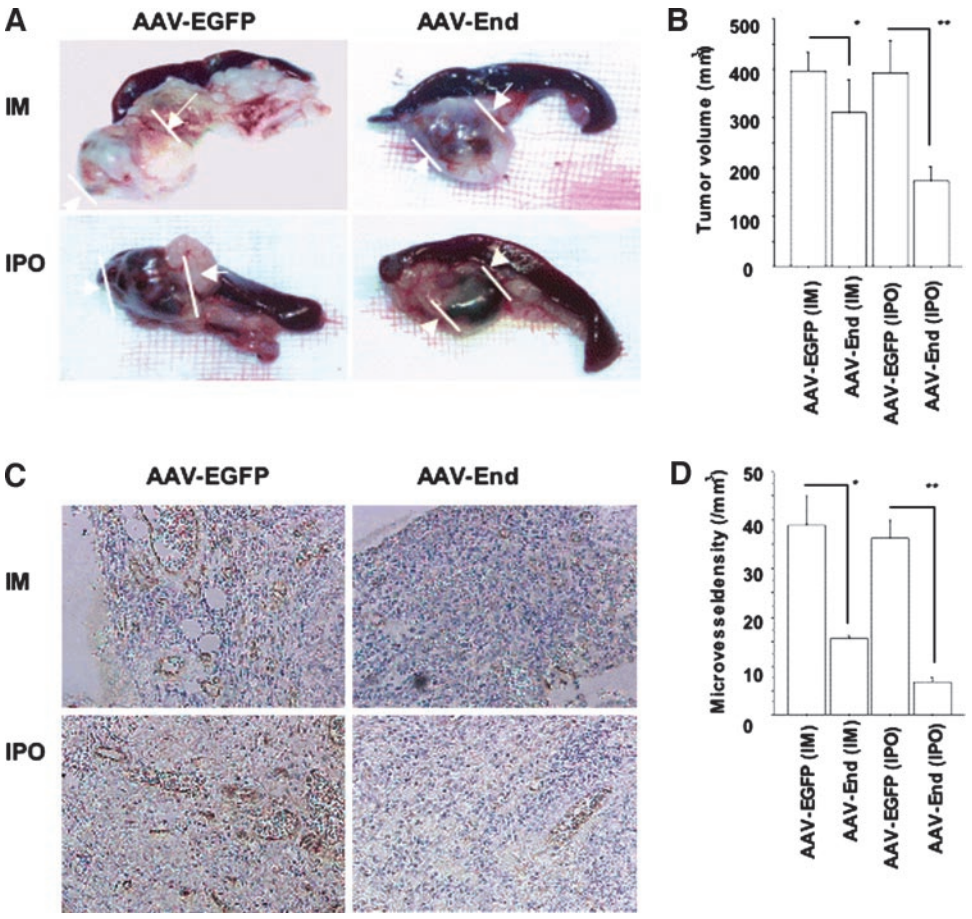

Fig. 4. Effects of AAV-mediated endostatin expression on pancreatic tumor growth. The mean sizes (*B*) of primary pancreatic tumors (*A*) were measured 21 days after tumor inoculation (42 days after vector administration; $n = 4$). *, $P > 0.05$; **, $P < 0.01$. Primary pancreatic tumors were immunostained with anti-von Willebrand factor antibody (*C*), and microvessel density was measured (*D*; $n = 4$). *, $P < 0.05$; **, $P < 0.01$. *IM*, intramuscular injection; *IPO*, intraportal injection.

DISCUSSION

In the present study, we compared the intramuscular and intraportal routes of AAV vector administration in terms of the relative potency of antiangiogenic gene therapy for pancreatic cancer and liver metastasis using an orthotropic animal model. AAV vectors have often been injected intramuscularly to systemically deliver various types of secretable protein molecules because of the easy accessibility and decreased invasiveness of this route (22, 28–30). Another advantage of muscle-directed gene therapy is minimal spill-over of the injected vectors (22). Our experimental system confirmed that the vector sequence is localized at the injection site. Compared with the intramuscular route, intraportal injection is more invasive and is likely to be more hazardous for liver function. Despite these potential disadvantages, liver-directed gene transfer has been postulated to achieve more efficient transgene expression (28, 29, 31). In our experiments with immunocompetent hamsters, we indeed confirmed the reported finding that expression mediated by AAV is more efficient in the liver than in muscle.

The antitumor effects of endostatin appear to be closely correlated with its serum concentration. Low levels of serum endostatin after AAV-IM injection certainly reduced the number of metastases and the incidence of hemorrhagic ascites. However, primary tumor growth was not evidently inhibited. In contrast, intraportal injection of AAV resulted in high levels of serum endostatin followed by significant inhibition of both primary tumor growth and the development of metastasis. Another factor that needs to be considered here is that the concentration of endostatin may be much higher in the liver, where the gene is expressed, than in serum. Liver-directed gene transfer of the angiostatic gene is a valuable treatment option for primary liver tumors and liver metastases.

The important point of this work is that we used an orthotopic animal model of metastatic pancreatic cancer. Heterotopic graft models used in previous studies ignore the histologic and anatomic specificity of the organs of the primary as well as the distant sites (32). Consequently, these studies do not adequately serve as preclinical trials for human gene therapy. Orthotopic grafts are essential to evaluation of the routes of gene transfer, especially the assessment of metastasis. The disadvantage of this model is that PGHAM-1 cells grow and invade very quickly. Under the experimental conditions in this investigation, all transplant-treated hamsters died at about 4 weeks after cell inoculation, irrespective of treatment. The statistically significant inhibition of primary tumor growth and metastasis did not immediately impact the survival rate of the treated animals. The overall effects of antiangiogenic cancer therapy must therefore be further studied using a different model system in which transplanted cancer cells grow more slowly, ideally in a manner consistent with naturally occurring human cancer cells.

To achieve the antiangiogenic state in model animals, we used classical AAV serotype 2 vectors in this experiment. The advantages of AAV vectors include a lack of pathogenicity, low immunogenicity, stable expression from either the integrated or episomal genome, and the ability to transduce growth-arrested cells (17, 33, 34). One problem is that it takes several weeks to reach the maximal level of transgene expression. Therefore, to evaluate the efficacy of cancer gene therapy in a transplant-treated model animal, the AAV vector must be injected before tumor inoculation (35–37). The disadvantages of AAV serotype 2 vectors include a relatively low transduction efficiency and the difficulty of large-scale production. Recently, many different serotypes of AAV have been characterized (38), and AAV serotype 1 vectors have been shown to be highly efficient in gene transfer into both muscle and liver in animal models (39). AAV serotype 1 vectors may turn out to be the vector of

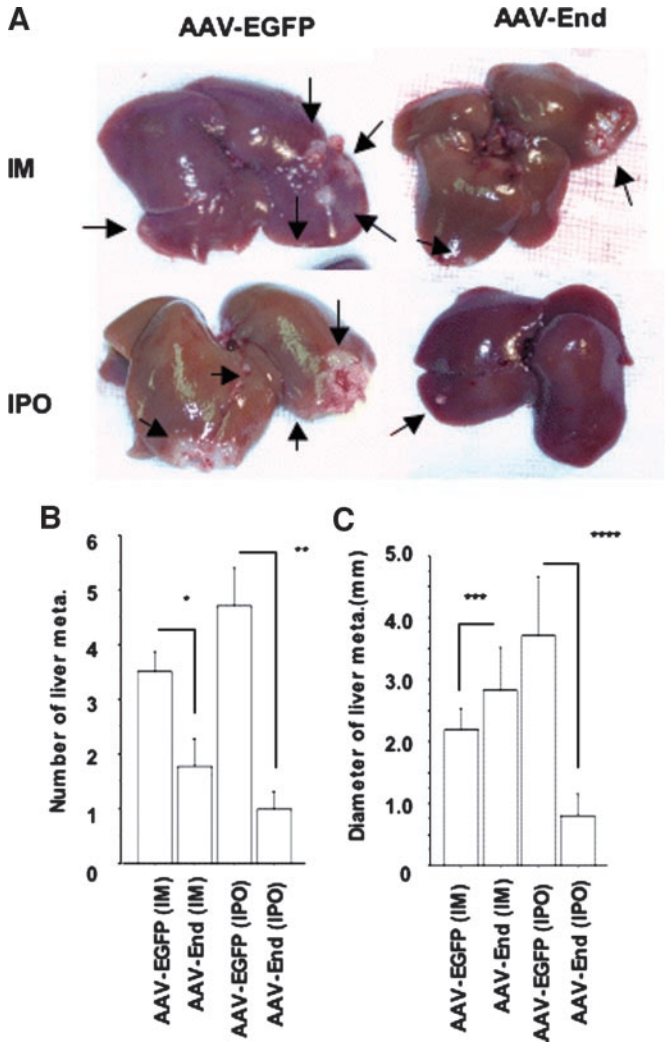

Fig. 5. Effects of AAV-mediated endostatin expression on liver metastases. Numbers (*B*) and sizes (*C*) of metastatic tumors in the liver (*A*) were measured. *Arrows* indicate the location of liver metastases ($n = 4$). *, $P < 0.05$; **, $P < 0.01$; ***, $P > 0.05$; ****, $P < 0.05$. *IM*, intramuscular injection; *IPO*, intraportal injection.

choice for additional preclinical and clinical studies of systemic antiangiogenic cancer gene therapy.

ACKNOWLEDGMENTS

We thank Manami Okabe and Motoko Yamamoto for excellent technical assistance. In addition, we thank Takayuki Aimoto, Munehisa Fukuhara, and Makoto Hiroi for advice and expertise.

REFERENCES

1. Gordis L, Gold EB. Epidemiology of pancreatic cancer. World J Surg 1984;8:808–21.
2. Staley CA, Lee JE, Cleary KR, et al. Preoperative chemoradiation, pancreaticoduodenectomy, and intraoperative radiation therapy for adenocarcinoma of the pancreatic head. Am J Surg 1996;171:118–24.
3. Williamson RC. Pancreatic cancer: the greatest oncological challenge. Br Med J 1988;296:445–6.
4. Tsiotos GG, Farnell MB, Sarr MG. Are the results of pancreatectomy for pancreatic cancer improving? World J Surg 1999;23:913–9.
5. Gunji Y, Ochiai T, Shimada H, Matsubara H. Gene therapy for cancer. Surg Today 2000;30:967–73.
6. Dranoff G, Jaffee E, Lazenby A, et al. Vaccination with irradiated tumor cells engineered to secrete murine granulocyte-macrophage colony-stimulating factor stimulates potent, specific, and long-lasting anti-tumor immunity. Proc Natl Acad Sci USA 1993;90:3539–43.
7. Foa R, Guarini A, Gansbacher B. IL2 treatment for cancer: from biology to gene therapy. Br J Cancer 1992;66:992–8.
8. Tahara H, Lotze MT. Antitumor effects of interleukin-12 (IL-12): applications for the immunotherapy and gene therapy of cancer. Gene Ther 1995;2:96–106.
9. Chen CT, Lin J, Li Q, et al. Antiangiogenic gene therapy for cancer via systemic administration of adenoviral vectors expressing secretable endostatin. Hum Gene Ther 2000;11:1983–96.
10. Ding I, Sun JZ, Fenton B, et al. Intratumoral administration of endostatin plasmid inhibits vascular growth and perfusion in MCa-4 murine mammary carcinomas. Cancer Res 2001;61:526–31.
11. Yanagi K, Onda M, Uchida E. Effect of angiostatin on liver metastasis of pancreatic cancer in hamsters. Jpn J Cancer Res 2000;91:723–30.
12. Matsushita A, Onda M, Uchida E, Maekawa R, Yoshioka T. Antitumor effect of a new selective matrix metalloproteinase inhibitor, MMI-166, on experimental pancreatic cancer. Int J Cancer 2001;92:434–40.
13. O'Reilly MS, Boehm T, Shing Y, et al. Endostatin: an endogenous inhibitor of angiogenesis and tumor growth. Cell 1997;88:277–85.
14. Rehn M, Veikkola T, Kukk-Valdre E, et al. Interaction of endostatin with integrins implicated in angiogenesis. Proc Natl Acad Sci USA 2001;98:1024–9.
15. Dhanabal M, Ramchandran R, Waterman MJ, et al. Endostatin induces endothelial cell apoptosis. J Biol Chem 1999;274:11721–6.
16. Herzog RW, Hagstrom JN, Kung SH, et al. Stable gene transfer and expression of human blood coagulation factor IX after intramuscular injection of recombinant adeno-associated virus. Proc Natl Acad Sci USA 1997;94:5804–9.
17. Kaplitt MG, Leone P, Samulski RJ, et al. Long-term gene expression and phenotypic correction using adeno-associated virus vectors in the mammalian brain. Nat Genet 1994;8:148–54.
18. Kessler PD, Podsakoff GM, Chen X, et al. Gene delivery to skeletal muscle results in sustained expression and systemic delivery of a therapeutic protein. Proc Natl Acad Sci USA 1996;93:14082–7.
19. Koeberl DD, Alexander IE, Halbert CL, Russell DW, Miller AD. Persistent expression of human clotting factor IX from mouse liver after intravenous injection of adeno-associated virus vectors. Proc Natl Acad Sci USA 1997;94:1426–31.
20. Samulski RJ, Chang LS, Shenk T. Helper-free stocks of recombinant adeno-associated viruses: normal integration does not require viral gene expression. J Virol 1989;63:3822–8.
21. Blezinger P, Wang J, Gondo M, et al. Systemic inhibition of tumor growth and tumor metastases by intramuscular administration of the endostatin gene. Nat Biotechnol 1999;17:343–8.
22. Takahashi H, Hirai Y, Migita M, et al. Long-term systemic therapy of Fabry disease in a knockout mouse by adeno-associated virus-mediated muscle-directed gene transfer. Proc Natl Acad Sci USA 2002;99:13777–82.
23. Tamayose K, Hirai Y, Shimada T. A new strategy for large-scale preparation of high-titer recombinant adeno-associated virus vectors by using packaging cell lines and sulfonated cellulose column chromatography. Hum Gene Ther 1996;7:507–13.
24. Igarashi T, Miyake K, Kato K, et al. Lentivirus-mediated expression of angiostatin efficiently inhibits neovascularization in a murine proliferative retinopathy model. Gene Ther 2003;10:219–26.
25. Ferrari FK, Samulski T, Shenk T, Samulski RJ. Second-strand synthesis is a rate-limiting step for efficient transduction by recombinant adeno-associated virus vectors. J Virol 1996;70:3227–34.
26. Fisher KJ, Gao GP, Weitzman MD, et al. Transduction with recombinant adeno-associated virus for gene therapy is limited by leading-strand synthesis. J Virol 1996;70:520–32.
27. Yamamura S, Onda M, Uchida E. Two types of peritoneal dissemination of pancreatic cancer cells in a hamster model. Nippon Ika Daigaku Zasshi 1999;66:253–61.
28. Nathwani AC, Davidoff A, Hanawa H, et al. Factors influencing in vivo transduction by recombinant adeno-associated viral vectors expressing the human factor IX cDNA. Blood 2001;97:1258–65.
29. Zhou S, Murphy JE, Escobedo JA, Dwarki VJ. Adeno-associated virus-mediated delivery of erythropoietin leads to sustained elevation of hematocrit in nonhuman primates. Gene Ther 1998;5:665–70.
30. Song S, Morgan M, Ellis T, et al. Sustained secretion of human alpha-1-antitrypsin from murine muscle transduced with adeno-associated virus vectors. Proc Natl Acad Sci USA 1998;95:14384–8.
31. Xiao W, Berta SC, Lu MM, et al. Adeno-associated virus as a vector for liver-directed gene therapy. J Virol 1998;72:10222–6.
32. Egami H, Tomioka T, Tempero M, Kay D, Pour PM. Development of intrapancreatic transplantable model of pancreatic duct adenocarcinoma in Syrian golden hamsters. Am J Pathol 1991;138:557–61.
33. Nakai H, Iwaki Y, Kay MA, Couto LB. Isolation of recombinant adeno-associated virus vector-cellular DNA junctions from mouse liver. J Virol 1999;73:5438–47.
34. Chao H, Samulski R, Bellinger D, et al. Persistent expression of canine factor IX in hemophilia B canines. Gene Ther 1999;6:1695–704.
35. Shi W, Teschendorf C, Muzyczka N, Siemann DW. Adeno-associated virus-mediated gene transfer of endostatin inhibits angiogenesis and tumor growth in vivo. Cancer Gene Ther 2002;9:513–21.
36. Ma HI, Guo P, Li J, et al. Suppression of intracranial human glioma growth after intramuscular administration of an adeno-associated viral vector expressing angiostatin. Cancer Res 2002;62:756–63.
37. Davidoff AM, Nathwani AC, Spurbeck WW, et al. rAAV-mediated long-term liver-generated expression of an angiogenesis inhibitor can restrict renal tumor growth in mice. Cancer Res 2002;62:3077–83.
38. Chao H, Liu Y, Rabinowitz J, et al. Several log increase in therapeutic transgene delivery by distinct adeno-associated viral serotype vectors. Mol Ther 2000;2:619–23.
39. Rabinowitz JE, Rolling F, Li C, et al. Cross-packaging of a single adeno-associated virus (AAV) type 2 vector genome into multiple AAV serotypes enables transduction with broad specificity. J Virol 2002;76:791–801.